

This is the accepted manuscript made available via CHORUS. The article has been published as:

Quantum Control of the Spin-Orbit Interaction Using the Autler-Townes Effect

E. H. Ahmed, S. Ingram, T. Kirova, O. Salihoglu, J. Huennekens, J. Qi, Y. Guan, and A. M. Lyra

Phys. Rev. Lett. **107**, 163601 — Published 11 October 2011

DOI: [10.1103/PhysRevLett.107.163601](https://doi.org/10.1103/PhysRevLett.107.163601)

Quantum Control of the Spin-Orbit Interaction Using the Autler-Townes Effect

E. H. Ahmed,* S. Ingram, O. Salihoglu, Y. Guan, and A. M. Lyyra

Department of Physics, Temple University, Philadelphia, Pennsylvania 19122

T. Kirova

*Department of Physics, Temple University, Philadelphia, Pennsylvania 19122 and
National Institute for Theoretical Physics (NITheP), Stellenbosch 7600, South Africa*

J. Huennekens

Department of Physics, Lehigh University, Bethlehem, Pennsylvania 18015

J. Qi

Department of Physics and Astronomy, Penn State University, Berks Campus, Reading, Pennsylvania 19610

(Dated: August 2, 2011)

We have demonstrated quantum control of the spin-orbit interaction based on the Autler-Townes (AC Stark) effect in a molecular system using a cw optical field. We show that the enhancement of the spin-orbit interaction between a pair of weakly interacting singlet-triplet rovibrational levels, $G^1\Pi_g(v=12, J=21, f) \sim 1^3\Sigma_g^-(v=1, N=21, f)$, separated by 750 MHz in the lithium dimer, depends on the Rabi frequency (laser power) of the control laser.

PACS numbers: 42.50.Hz, 31.15.aj, 33.40.+f

The interaction between the spin and the orbital angular momenta (spin-orbit interaction) of the electron in an atom or a molecule often can be neglected or treated as a perturbation. However, when relativistic effects are not negligible, the spin-orbit interaction must be taken into account. It can cause mixing of electronic states of different spin-multiplicity, with the degree of mixing dependent on the strength of the spin-orbit interaction as well as the energy separation between the interacting states. It is also well known that, in the presence of strong electromagnetic fields, the energy levels in atoms or molecules experience shifts in their positions due to the Autler-Townes (AT) effect [1]. Thus control of the spin-orbit interaction can be realized using resonant or non-resonant laser fields as an external control mechanism. Several recent theoretical studies have been devoted to this subject [2–5].

Specific possible applications of quantum control of the spin-orbit interaction include enhancing the rate of population transfer to otherwise "dark" states, either by increasing the mixing between existing perturbed pairs of levels, or by creating mixed levels out of previously unmixed ones. In alkali molecules, states with mixed character (i.e. singlet and triplet) have been used as "gateways" or "windows" for accessing states with different spin character than the ground state [6–9]. Such perturbed levels have also been used as intermediate levels in the transfer of cold molecules formed at long range in the triplet $a^3\Sigma^+$ state to deeply bound levels of the singlet $X^1\Sigma^+$ ground state [10–14]. Thus, the ability to enhance the mixing of the spin character of singlet-triplet pairs of states could be used to improve the transfer rates in such schemes. Also there is a great deal of interest in controlling photochemical reactions and intersystem crossings by means of optical fields. For example, control of the chemical reaction potential energy surface using the non-resonant dynamic Stark effect has been demonstrated [15]. In principle, this control scheme could also be used in experiments that investigate the role of electron spin in entrance-channel controlled and excited state reactive collisions. Another possible application of control of the spin-orbit interaction with external fields is preparation of optical spin switches [3, 16–18].

In this work we demonstrate all-optical control of the spin-orbit interaction using the lithium dimer ($^7\text{Li}_2$) and a narrow band cw laser as the control field. The small linewidth (0.5 MHz) of the cw control laser allows the experiments to be performed state selectively using a specific singlet-triplet pair of rovibrational levels mixed by the spin-orbit interaction. We chose to work with $^7\text{Li}_2$, since for molecules with light nuclei, the spin and orbital angular momenta are weakly coupled and therefore the spin-orbit interaction is small. Thus the interacting levels can lie very close in energy without being significantly mixed. We use the $G^1\Pi_g(v=12, J=21, f) \sim 1^3\Sigma_g^-(v=1, N=21, f)$ pair of rovibrational levels (denoted as $|S\rangle \sim |T\rangle$, see Fig. 1), which are only separated by $\delta_{SO} = 750\text{MHz}$, as is evident from Fig. 2. In the absence of a control field, the nominally singlet (triplet) level has 87% singlet (triplet) and 13% triplet (singlet) character, determined using the ratios of the intensities from OODR laser excitation scans of the triplet and singlet peaks as described in [19]. The $1^3\Sigma_g^-$ electronic state has negligible hyperfine structure [20], and thus the predominantly triplet state $1^3\Sigma_g^-(v=1, N=21, f)$ can be considered to be a single level in the analysis.

The $^7\text{Li}_2$ dimers were generated in a heat pipe oven loaded with Lithium metal heated to a temperature of 850 K

(estimated from the Doppler linewidth of a single laser excitation). Argon at a pressure of about 150 mTorr was used as a buffer gas. Argon and lithium atom densities were sufficiently low that level changing collisions can be neglected. The excitation scheme used in the experiment is depicted in Fig. 1. The lasers used were Coherent 699-29 narrow band tunable ring dye lasers. The pump (L_1) and probe (L_2) lasers counterpropagated through the oven. The control laser (L_3) copropagated with the pump laser. The pump and probe laser powers were kept as low as possible while maintaining a good signal to noise ratio; $P_1 = 100 \mu\text{W}$ and $P_2 = 2.5 \text{ mW}$. The spot radii of the pump and probe lasers ($r_1 = 125 \mu\text{m}$ and $r_2 = 130 \mu\text{m}$) were chosen to be about half that of the control laser ($r_3 = 230 \mu\text{m}$). Thus only molecules that interact with the central portion of the control laser Gaussian spatial profile (TEM_{00}) were probed, thereby ensuring control laser electric field homogeneity in the interaction region.

In the experiment we have observed the spin character of the mixed pair of levels $|S\rangle \sim |T\rangle$ by simultaneously recording fluorescence from them to lower lying singlet and triplet levels (see Fig. 1). In order to monitor the triplet character, we detected fluorescence to a few lower lying rovibrational levels of the $b^3\Pi_u$ electronic state (collectively labeled $|5\rangle$ in Fig. 1), around 450nm, with a PMT mounted on one of the side arms of the heatpipe. To prevent the yellow and red laser scatter from saturating the PMT, blue band pass glass filter was placed in front of the photocathode. Because of spectral congestion, we chose to monitor the singlet character by observing fluorescence to a specific $A^1\Sigma_u^+$ rovibrational level, level $|4\rangle$ in Fig. 1, at 559.4nm using a SPEX 1404 double grating monochromator (equipped with a cooled PMT) in the role of a narrow band pass filter. The pump laser was mechanically modulated and the signal from each PMT was amplified using a lock-in amplifier.

To model theoretically the experimental results and to confirm the nature of the observed fluorescence line shapes, we have followed the theoretical framework introduced in [2] and the standard density matrix formalism [21]. The evolution of the density matrix ρ of our system is governed by the equation of motion

$$\frac{\partial \rho}{\partial t} = -\frac{i}{\hbar}[H, \rho] + \text{relaxation terms}, \quad (1)$$

where *relaxation terms* account for physical processes such as spontaneous decay of levels, collisions, etc. [21].

The total Hamiltonian H of the system can be expressed as the sum of three parts $H = H_{mol} + H_{SO} + H_{int}$. The Hamiltonian of the unperturbed molecule, H_{mol} , is diagonal in the basis set of the unperturbed molecular states and can be expressed as $H_{mol} = \sum_k \varepsilon_k |k\rangle\langle k|$, where the ε_k are its eigenvalues, and the levels are labeled as in Fig. 1. Because the spin-orbit interaction in $^7\text{Li}_2$ ($\sim 0.1 \text{ cm}^{-1}$) is much smaller than the typical spacing between the individual rovibrational levels in the electronic states ($\sim 20 \text{ cm}^{-1}$ at $J = 20$) we consider that the perturbation H_{SO} mixes only the closely spaced pair of unperturbed pure singlet $|S_0\rangle$ and pure triplet $|T_0\rangle$ states (eigenstates of H_{mol}). The result of the spin-orbit perturbation as shown in Fig. 1 is the creation of the mixed states $|S\rangle$ and $|T\rangle$ given by $|S\rangle = \alpha|S_0\rangle - \beta|T_0\rangle$ and $|T\rangle = \alpha|T_0\rangle + \beta|S_0\rangle$, where α and β are mixing coefficients and $\alpha^2 + \beta^2 = 1$ ($\alpha^2 = 0.87$ and $\beta^2 = 0.13$). The spin-orbit interaction part of the Hamiltonian of the system, H_{SO} , can be expressed simply as $H_{SO} = \alpha\beta\delta_{SO}$ [7, 19], where δ_{SO} is the separation in energy between the mixed levels $|S\rangle$ and $|T\rangle$. Finally, once the laser fields are turned on, we must include H_{int} in the Hamiltonian. H_{int} represents the interaction of the molecule with the optical fields, and in the dipole approximation has the form $-\vec{\mu} \cdot \vec{E}$, where $\vec{\mu}$ is the transition dipole moment between the levels coupled by a laser with electric field \vec{E} .

We solve Eq. (1) under the steady state condition in the interaction picture where the Hamiltonian of the system, H_I , after applying the rotating wave approximation, has the explicit form

$$\begin{aligned} \frac{H_I}{\hbar} = & -\delta_1|2\rangle\langle 2| - (\delta_1 + \delta_2)|S_0\rangle\langle S_0| - (\delta_1 + \delta_2 - \delta_3)|3\rangle\langle 3| \\ & - (\delta_1 + \delta_2 + \delta_{SO}^0)|T_0\rangle\langle T_0| + \frac{\Omega_1}{2}(|2\rangle\langle 1| + |1\rangle\langle 2|) \\ & + \frac{\Omega_2}{2}(|S_0\rangle\langle 2| + |2\rangle\langle S_0|) + \frac{\Omega_3}{2}(|3\rangle\langle S_0| + |S_0\rangle\langle 3|) \\ & + \alpha\beta\delta_{SO}(|S_0\rangle\langle T_0| + |T_0\rangle\langle S_0|) \end{aligned} \quad (2)$$

which is written in a basis of levels that are unperturbed by either the optical fields or the spin-orbit interaction. Here $\delta_i \equiv \Delta_i \pm k_i v_z$ is the velocity dependent detuning of the i^{th} laser and $\Delta_i \equiv \omega_i - \omega_{i,res}$ are the detunings for molecules at rest in the lab frame. ω_i is the frequency of the i^{th} laser and $\omega_{i,res}$ is the resonance transition frequency between the corresponding unperturbed levels. δ_{SO}^0 is the splitting of the unperturbed levels (note $\delta_{SO}^0 = (\alpha^2 - \beta^2)\delta_{SO}$). $\Omega_i = \mu_i E_i / \hbar$ is the Rabi frequency of the i^{th} laser.

When only the weak pump and the probe lasers are present, the laser interactions are minimal, and the upper levels are essentially the perturbed spin-orbit pair $|S\rangle$ and $|T\rangle$. The fluorescence excitation spectrum of the $|S\rangle \sim |T\rangle$

system as a function of the probe laser detuning shows a two peak pattern as expected (see Fig. 2). We have used this relatively simple two laser excitation spectrum to test the theoretical model. As Fig. 2 shows, there is very good agreement between the two experimental traces (solid lines) and the simulations (dotted lines). The parameters used in the model were taken either from independent measurements or from theoretical calculations.

When the control field is turned on, resonantly coupling states $|S\rangle$ and $|3\rangle$, we observe the nominally singlet peak splitting into two components due to the AT effect as shown in Fig. 3. The separation between the two components, labeled $|S, -AT\rangle$ and $|S, +AT\rangle$ (see Fig. 1), of the split singlet peak is determined by the Rabi frequency of the control laser. The $|S, -AT\rangle$ component of the pair is shifted closer to the nearby $|T\rangle$ state which leads to stronger spin-orbit interaction between them. As a result, the $|S, -AT\rangle$ component acquires more triplet character, while the $|T\rangle$ level shifts slightly and acquires more singlet character (transformed into the modified state $|T'\rangle$), demonstrated by the significant increase in the area of the nominally $1^3\Sigma_g^-(v=1, N=21, f)$ peak in the singlet detection channel as can be seen in Fig. 3b. At the same time the singlet character of the $|S, +AT\rangle$ component is enhanced due to its increased separation from the $|T\rangle$ state (which decreases its mixing with the triplet level). The two AT split components of the predominantly singlet level now have different amounts of singlet and triplet character from each other. This results in an asymmetric line shape of the AT pair intensity distribution, in both the singlet and triplet detection channels, as is evident from Fig. 3a. We note that asymmetric AT split intensity distributions can also be observed when the control field is slightly off resonance. But in the present case, the fact that the asymmetry is in the opposite sense for the singlet and triplet channels shows that the asymmetry observed here is due to the different amount of mixing of the two components of the AT pair with the $|T\rangle$ state.

To estimate how the character of the nominally triplet level $1^3\Sigma_g^-(v=1, N=21, f)$ changes in the presence of the control laser we consider that state $|T'\rangle$ is a superposition of the unperturbed levels $|T_0\rangle$, $|S_0\rangle$, and $|3\rangle$. We write $|T'\rangle = \alpha'|T_0\rangle + \beta'|S_0\rangle + \gamma'|3\rangle$ where α' , β' , and γ' are the mixing coefficients with the control laser on. The spin-orbit interaction only mixes $|T_0\rangle$ with $|S_0\rangle$ but not with $|3\rangle$ due to the spin-orbit selection rules ($g \leftrightarrow u$, and $\Delta J = 0$). Thus the mixing of level $|3\rangle$ character into state $|T'\rangle$ only occurs via the relatively small $\beta'|S_0\rangle$ component in the latter. Consequently in our simple model, we set $\gamma' \approx 0$. Using $I(t)_{|T'\rangle}/I(s)_{|T'\rangle} = \varepsilon\alpha'^2/\beta'^2$, where $I(t)_{|T'\rangle}$ and $I(s)_{|T'\rangle}$ are the triplet and singlet channel fluorescence intensities (peak areas) of state $|T'\rangle$ in Fig. 3a, and the normalization condition $\alpha'^2 + \beta'^2 = 1$, we calculate $\alpha'^2 = 0.72$ and $\beta'^2 = 0.28$. The relative efficiency of detecting singlet vs. triplet fluorescence ε is calculated from the data in Fig. 2 following Ref. [19]. By comparing the values of β^2 and β'^2 , we see that the singlet character of the nominally triplet state has been enhanced by more than a factor of two, from 13% to 28%, when the control laser with power of 700 mW is turned on.

By varying the amplitude of the control laser field one can enhance or reduce the spin-orbit interaction. The control effect depends on the magnitude of the induced shift in the position of the levels relative to the natural spin-orbit splitting δ_{SO} . Fig. 4 shows probe laser scans with detection of the singlet fluorescence for a number of power levels of the control laser. At low power values (100 mW), there is no measurable enhancement of the mixing and the AT split components are symmetric. Increasing the control laser power leads to an increase in the mixing. The leftmost peak, corresponding to the level with primarily $1^3\Sigma_g^-(v=1, N=21, f)$ (triplet) character grows in the singlet detection channel and the AT split pair of peaks becomes more and more asymmetric. At higher control laser powers (500-700 mW) a shift in the position as well as broadening of the $1^3\Sigma_g^-(v=1, N=21, f)$ peak can be observed due to the non-resonant AC-Stark effect of the control laser and the increased spin-orbit interaction of $|T'\rangle$ with the $|S, -AT\rangle$ component.

In summary, we have demonstrated all-optical frequency domain quantum control of the spin-orbit interaction in a molecular system. We observed that the application of a strong control field to the singlet component of a $^7\text{Li}_2\ G^1\Pi_g \sim 1^3\Sigma_g^-$ singlet-triplet weakly mixed pair of rovibrational levels leads to a significant enhancement of their mixing, and consequently to a significant change in their quantum state characters. We were able to enhance the singlet character of the predominantly triplet state from 13% to 28%. The change in magnitude of the spin-orbit interaction depends on the Rabi frequency (laser power) of the control laser. The results of our proof-of-concept demonstration can be extended to experiments with stronger control fields, bearing in mind that the control laser does not need to be resonant with a populated ground state level. This feature is particularly useful for mitigating the effects of multiphoton ionization in such experiments.

We gratefully acknowledge valuable discussions with Dr. F. Spano on the theoretical model and financial support from NSF Grants PHY 0555608, PHY 0855502, and PHY 0968898.

* Corresponding author; email: erahmed@temple.edu

- [1] C. H. Townes and A. L. Schawlow, *Microwave Spectroscopy*, McGraw-Hill, London (1955).
- [2] T. Kirova and F. C. Spano, *Phys. Rev. A* **71**, 063816 (2005).
- [3] M. V. Korolkov and J. Manz, *J. of Chem. Phys.* **120**, 11522 (2004).
- [4] J. Gonzalez-Vazquez, et al., *Chem. Phys. Lett.* **431**, 231 (2006).
- [5] J. Gonzalez-Vazquez, et al., *J. of Chem. Phys.* **125**, 124315 (2006).
- [6] L. Li and R. W. Field, *J. of Phys. Chem.* **87**, 3020 (1983).
- [7] X. Xie and R. W. Field, *Chem. Phys.* **99**, 337 (1985).
- [8] L. Li, et al., *J. of Phys. Chem.* **97**, 8835 (1992).
- [9] A. M. Lyyra, et al., *Phys. Rev. Lett.* **66**, 2724 (1991).
- [10] J. M. Sage, et al., *Phys. Rev. Lett.* **94**, 203001 (2005).
- [11] K. K. Ni, et al., *Science* **322**, 231 (2008).
- [12] J. G. Danzl, et al., *Science* **321**, 1062 (2008).
- [13] M. Viteau, et al., *Science* **321**, 232 (2008).
- [14] S. Ghosal, et al., *New J. of Phys.* **11**, 055011 (2009).
- [15] B. J. Sussman, et al., *Science* **314**, 278 (2006).
- [16] R. Gomez-Abal and W. Hubner, *Phys. Rev. B* **65**, 195114 (2002).
- [17] K. Satitkovitchai, et al., *Phys. Rev. B* **72**, 045116 (2005).
- [18] I. R. Sola, et al., *Phys. Rev. A* **74**, 043418 (2006).
- [19] H. Q. Sun and J. Huennekens, *J. of Chem. Phys.* **97**, 4714 (1992).
- [20] A. Yiannopoulou, et al., *J. of Chem. Phys.* **101**, 3581 (1994). R. J.
- [21] S. Stenholm, *Foundations of Laser Spectroscopy*, Wiley Interscience, New York (1984).
- [22] P. Kusch and M. M. Hessel, *J. of Chem. Phys.* **67**, 586 (1977).
- [23] K. Urbanski, et al., *J. of Chem. Phys.* **109**, 912 (1998).
- [24] O. Salihoglu, et al., *J. of Chem. Phys.* **129**, 174301 (2008).
- [25] Private communication with G.-H. Jeung.
- [26] R. J. Le Roy, U. of Waterloo Chem. Phys. Report No. CP663 (2007).

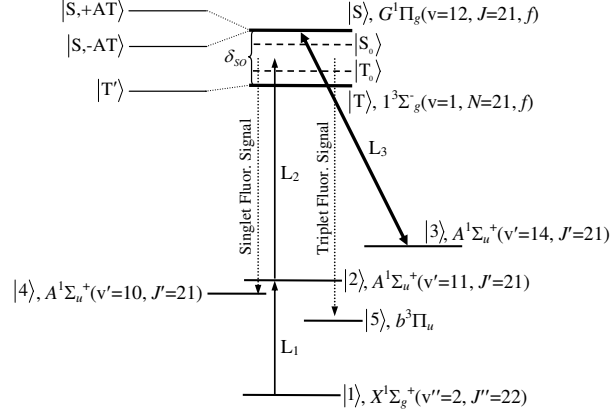


FIG. 1: Thermal population in level $|1\rangle$ is excited to level $|2\rangle$ by the weak pump laser L_1 (15810.158 cm^{-1}), and then further excited by tuning the weak probe field L_2 to the mixed pair of levels $|T\rangle$ and $|S\rangle$, with resonances at 17666.136 cm^{-1} and 17666.162 cm^{-1} , respectively. Laser L_3 is set on resonance with the $|S\rangle \leftrightarrow |3\rangle$ transition at 17026.872 cm^{-1} . Levels $|S_0\rangle$ and $|T_0\rangle$ are the 'pure' singlet and triplet basis states, respectively (unperturbed basis set). With the control laser on, $|S\rangle$ and $|T\rangle$ evolve into $|S, -AT\rangle$, $|S, +AT\rangle$, and $|T'\rangle$. The parameters $\mu_1 = 2.1$ D, $\mu_2 = 1.8$ D, $\mu_3 = 3.3$ D, $\tau_2=18.78$ ns, $\tau_{S_0}=16.21$ ns, $\tau_{T_0}=9.27$ ns, and $\tau_3=18.90$ ns were calculated from molecular data [20, 22–25] using LEVEL [26].

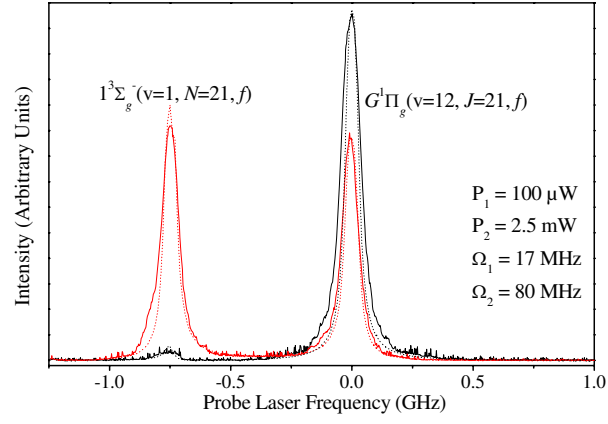


FIG. 2: OODR spectra recorded by monitoring the fluorescence to the $A^1\Sigma_u^+(v'=10, J'=21)$ level (singlet channel - black line) and to a few low lying rovibrational levels of the $b^3\Pi_u$ state (triplet channel - red line) as a function of the detuning of the probe laser. The control laser was blocked during these scans. The dotted lines represent simulations of the experimental spectra.

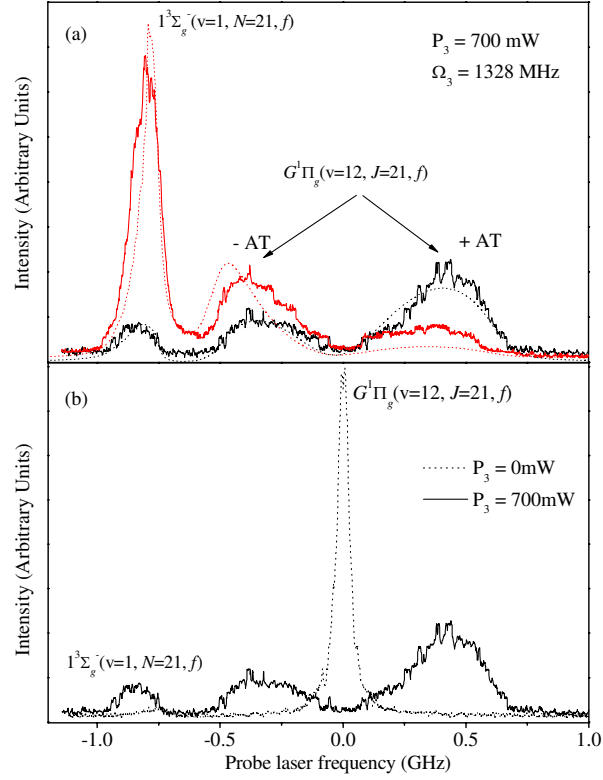


FIG. 3: (a) The singlet (black) and triplet (red) channel spectra recorded simultaneously in the presence of the control laser. Since the $|S, -AT\rangle$ component has acquired more triplet character (and the $|S, +AT\rangle$ component has lost triplet character) their intensities are asymmetric in opposite directions for the singlet and triplet signals. Dotted lines represent simulations. The parameters for L_1 and L_2 were the same as in Fig. 2. (b) Comparison of the singlet detection channel spectra with ($P_3 = 700$ mW) and without ($P_3 = 0$ mW) the control laser. It can be seen that the singlet character of the predominantly triplet level $1^3\Sigma_g^-(v=1, N=21, f)$ is dramatically enhanced by the presence of the control laser.

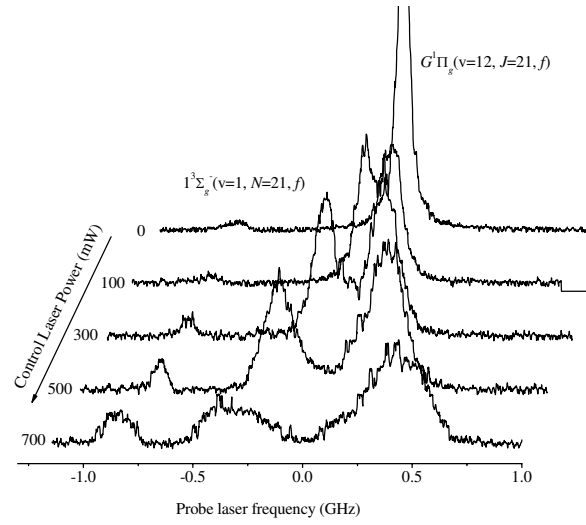


FIG. 4: Dependence of the singlet-triplet mixing and the magnitude of the AT splitting on the control laser power. The spectra were recorded by monitoring singlet fluorescence to the $A^1\Sigma_u^+(v'=10, J'=21)$ level. The leftmost peak in each spectrum corresponds to fluorescence from the level $|T'\rangle$ with primarily $1^3\Sigma_g^-(v=1, N=21, f)$ character while the peak(s) on the right correspond to fluorescence from the AT split pair of levels $|S, -AT\rangle$ and $|S, +AT\rangle$ with primarily $G^1\Pi_g(v=12, J=21, f)$ character.